

Experimental behavior of a magnetic field shield for an underground power line

J.R. Riba Ruiz¹, X. Alabern Morera²

¹ Department d'Enginyeria Elèctrica, UPC
EUETII-"L'Escola d'Adoberia"

Plaça del Rei 15, 08700 Igualada (Spain)
phone:+34 938 035300, fax:+34 938 031589, e-mail: jordi@euetii.upc.edu

² Department d'Enginyeria Elèctrica, UPC
C./ Colom 11, 08222 Terrassa (Spain)

phone: +34 937 398035, alabern@ee.upc.edu

Abstract

This paper describes the experimental behavior of a pure iron magnetic shield for a single-phase underground power line. We have built a 0,5 mm-thick 2 m-long cylindrical shell. The measures realized show that this shield is very effective in order to reduce the magnetic field generated by a single-phase power line placed inside the shield, just in its center.

It is well known that the relative magnetic permeability of ferromagnetic materials decreases sharply when magnetic fields intensities H are very weak (below 0,1 A/m) and when they are very strong (due to saturation phenomena). In these situations the shielding efficiency of these materials is dramatically reduced. This means that the selection of an adequate material to act as a magnetic field is decisive. In order to maximize the absorption losses, such a material must have a high magnetic permeability and a high electric conductivity when dealing with very weak magnetic fields. For these reasons we have selected the purified iron (with a pureness at least 99'95 %).

The ferromagnetic material of the shield (in the studied case is the pure iron) absorbs the magnetic field generated by the buried power line and just a very small portion of the magnetic field survives outside the shield. It is due that as the shield is made pure iron, which has a high electrical conductivity, the induced eddy generate a magnetic field opposed to the magnetic field generated by the power line. Due to the opposed magnetic field, the total magnetic field H outside the shield is reduced.

Key words

Magnetic shielding, magnetic field, soft ferromagnetic materials, absorption losses, power lines.

1. Introduction

In this work we have built a cylindrical shell that acts as a magnetic shield for an underground single-phase power line. We have measured its behavior by using a magnetic field meter.

It is well known that electrical machines and power lines create magnetic fields in their proximity. These magnetic fields are undesirable and can produce electromagnetic

interferences in the electric and electronic equipments placed in their surroundings. In June of 2001, IARC (International Agency for Research on Cancer) published a document^[1] explaining that *the pooled analyses of data from a number of well-conducted studies show a fairly consistent statistical association between a doubling of risk of childhood leukaemia and power-frequency (50 or 60 Hz) residential ELF magnetic field strengths above 0.4 μ Tesla*. But many other medical studies conclude that electric and magnetic fields generated by power lines are not harmful for human beings. Nowadays, the scientific community have not reached to a consensus about the possible harmful effects of magnetic fields on the human body. For these reasons and by applying the principle of caution, we think that it is very important to investigate the behavior of low-cost magnetic shielding materials, such as pure-iron and others in order to build inexpensive magnetic shields for power lines, power transforms, etc.

The magnetic fields generated by underground power lines have intensity values of some μ T in the vertical of the line (1 m above the floor surface). The magnetic field decreases sharply when the distance to the line increases. Magnetic fields generated by the power lines have very low intensities (about 1-10 μ T). It is well known that the relative magnetic permeability of ferromagnetic materials decreases sharply when magnetic fields intensities H are very weak (below 0,1 A/m) and when they are very strong (due to saturation phenomena). In these situations the shielding efficiency of these materials is dramatically reduced. This means that the selection of an adequate material to act as a magnetic field is decisive. Such a material must have a high magnetic permeability and a high electric conductivity when dealing with very weak magnetic fields in order to maximize the absorption losses.

For these reasons we have selected the purified iron^[1] (at least 99'95 % pureness) that combines a very high electric conductivity with high permeability values for low magnetic fields.

2. The electric and magnetic properties of pure-iron

In order to build the magnetic shield, we have selected the purified iron (99'95 % pureness). This is due to the fact that purified iron has a high magnetic permeability when dealing with weak magnetic field intensities and also has a high electric conductivity and reduced hysteresis losses.

Table I shows the pure-iron electric and magnetic properties.

TABLE I. Electric and magnetic properties for purified iron^[2].

Material	Purified Iron
Electric conductivity	$\sigma = 10^7$ S/m
Relative permeability (B = 2 mT)	$\mu_r = 5000$
Maximum relative permeability	$\mu_{r,max.} = 180000$
Skin depth ($\mu_r = 5000$)	$\delta = 0,32$ mm
Skin depth ($\mu_r = 180000$)	$\delta = 0,05$ mm
Hysteresis losses*	30 J/m ³
Density	7880 kg/m ³

* In magnetic saturation conditions

When dealing with a fixed frequency, the magnetic field reduction factor is very dependent on the skin depth δ . The skin depth is one of the most important factors to take into consideration when designing a magnetic field shield.

The skin depth can be calculated from the following expression:

$$\delta = 1 / \sqrt{\pi f \mu \sigma}$$

being f the electric network frequency expressed in Hz, μ the absolute permeability of the material of the shield expressed in H/m, and σ its electric conductivity expressed in $(\Omega.m)^{-1}$.

3. The magnetic shield and the magnetic field meter

The magnetic shield consists on a pure-iron cylindrical shell with a nominal thickness of 0,5 mm and an approximate external diameter of 30 cm, as shown in figure 1. The two conductors of the single-phase line are parallel and they are separated 18,25 cm.

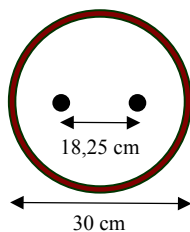


Figure 1. The magnetic shield geometry.

In order to measure the magnetic field, we have used a three-axis HIBOK EMF-829 magnetic field meter. This

meter measures the magnetic field in an orthogonal a three-axis system. It is based on three orthogonal sensors X, Y and Z and allows us to read the measured value in each single axis and also allows us to measure the RMS value of the three-dimensional magnetic field. This means that the measurement is independent of the spatial orientation of the meter.

The accuracy of the HIBOK EMF-829 magnetic field meter is $\pm 3\%$ and in the used scale of 20 μ T is 0,01 μ T. It has a broadband from 30 Hz to 2000 Hz and fulfills the CE standards.



Figure 2. The three-axis magnetic field meter.

4. Computation of the magnetic field of a single-phase line

It is well known that the magnetic field intensity of an infinite-long conductor that carries a current intensity I_i can be expressed as:

$$B = \frac{\mu_0 I_i}{2\pi r_i}$$

being

$$r_i = \sqrt{(x - x_i)^2 + (y - y_i)^2}$$

where (x,y) are the coordinates of the point where the magnetic field is being calculated, and (x_i,y_i) are the coordinates of the i -th conductor and $\mu_0 = 4\pi \cdot 10^{-7}$ N/A² is the magnetic permeability of the air.

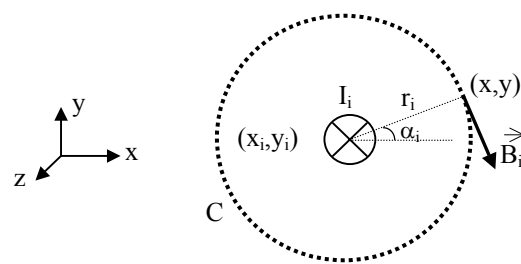


Figure 3. Axes and magnetic field created by an infinite conductor.

From figure 3 it can be deduced the vectorial expression of the magnetic field created by an infinite conductor as follows:

$$\vec{B}_i = \frac{\mu_0 I_i \varphi}{2\pi} \left(\frac{y - y_i}{r_i^2}, -\frac{x - x_i}{r_i^2}, 0 \right)$$

where φ is the phase-angle of the intensity. The I_i and B_i are alternating magnitudes and they must be expressed in RMS value.

When dealing with a single-phase line, it is to say two parallel conductors carrying identical intensities but with a difference of phase of 180° ($I_2 = -I_1 = -I$), the expression of the total magnetic field computed in the straight line placed in the vertical of $x = 0$ ($y_1 = y_2$, $r_1 = r_2 = \sqrt{x_1^2 + y^2}$) becomes:

$$\vec{B} = \frac{\mu_o I}{2\pi} \left(\frac{y-y_1}{r^2} - \frac{y-y_2}{r^2}, -\frac{x-x_1}{r^2} + \frac{x-x_2}{r^2}, 0 \right)$$

As $y_1 = y_2$, the former expression can be simplified as:

$$\vec{B} = \frac{\mu_o I}{2\pi r^2} (0, x_1 - x_2, 0) \quad (1)$$

5. The geometry of the experimental arrangement

In this work we study a 230V single-phase line, which carries an intensity of 54,4 A. As shows equation (1), the magnetic field strength in a given point of the space is directly proportional to the current intensity of the single-phase line.

Figure 4 shows the experimental arrangement built in order to measure the magnetic field in the vicinity of the magnetic field shield. As explained before, the total magnetic field has been measured in the straight line placed in the vertical of $x = 0$ (y axis in figure 4). The components of the experimental arrangement can't be made of iron or any ferromagnetic material because they could interfere the measurements.

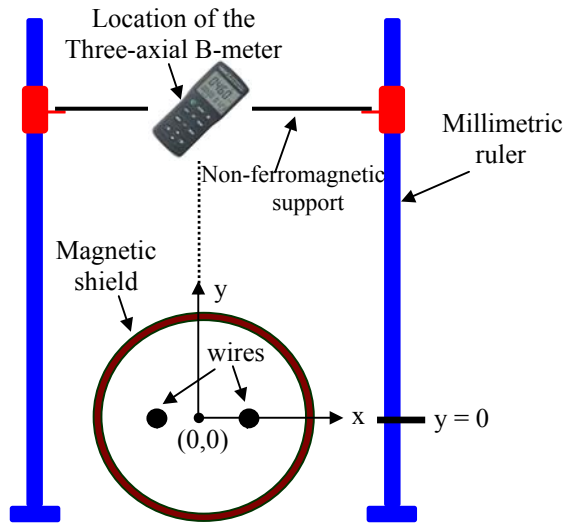


Figure 4. The experimental arrangement.

As shows figure 4, we have measured the magnetic field B in 15 different points placed in the $(0,y)$ axis.

In order to evaluate the efficiency of the magnetic field shield, the magnetic field reducing factor ($RF\%$) is defined as:

$$RF\% = 100 \cdot \frac{B_o - B}{B_o}$$

where B_o is the magnetic field intensity in any point of the space when the magnetic shield is not present, and B

is the magnetic field intensity in the same point when the shield is present. If due to the shield, the magnetic field is reduced, the values of the magnetic field reducing factor will be positive, but if there was an increment of the magnetic field, their values would be negative.

6. Calibration of the methodology

Before measuring the shield efficiency ($RF\%$), we have tested the methodology proposed in this work by comparing the magnetic field in the vicinity of the single-phase line obtained by using two methods: the first method consists on computing the magnetic field by applying equation (1) while second method consists on measuring the actual magnetic field by using the HIBOK EMF-829 meter.

Table II shows the values of the magnetic field by applying the two methods.

TABLE II. Computed and measured magnetic field intensities

y (m)	Computed B (μ T)	Measured B (μ T)	Error %
0.31	19.01	18.50	2.70
0.36	14.40	14.30	0.67
0.41	11.25	11.10	1.37
0.46	9.03	9.00	0.32
0.51	7.40	7.40	-0.04
0.56	6.17	6.20	-0.52
0.61	5.22	5.27	-0.97
0.66	4.47	4.45	0.51
0.71	3.87	3.89	-0.39
0.76	3.39	3.37	0.56
0.81	2.99	2.97	0.62
0.86	2.65	2.63	0.93
0.91	2.37	2.36	0.59
0.96	2.14	2.10	1.65
1.01	1.93	1.89	2.11

Figure 5 displays the magnetic field intensities shown in table II.

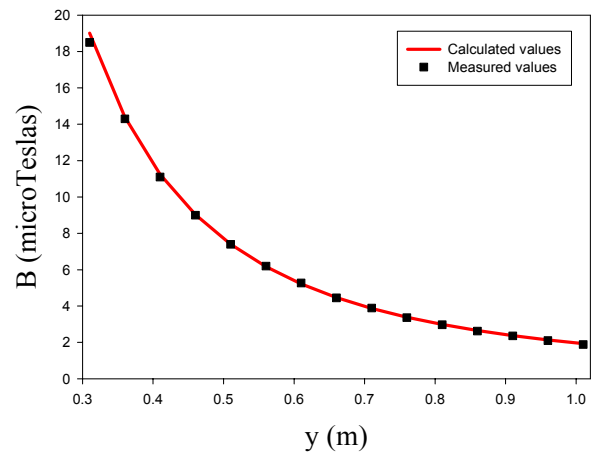


Figure 5. Computed and measured magnetic field intensities

From table II and figure 5 it can be deduced that the measured values of the magnetic field intensity are very similar to the computed values. This means that we can deduce that the proposed methodology is valid in order to measure the shielding efficiency of the pure-iron magnetic shield.

7. Results

In this heading we present the measured magnetic field intensities when a 0,5 mm-thick cylindrical pure-iron magnetic field is present.

Tables III shows the magnetic field intensities, measured in the straight line placed in the vertical of $x = 0$.

TABLE III. Measured magnetic field values and the reducing factor.

y (m)	B_o (μ T) (without shield)	B (μ T) (with shield)	RF%
0.31	18.50	5.23	71.73
0.36	14.30	4.11	71.26
0.41	11.10	3.24	70.81
0.46	9.00	2.62	70.89
0.51	7.40	2.20	70.27
0.56	6.20	1.85	70.16
0.61	5.27	1.56	70.40
0.66	4.45	1.35	69.66
0.71	3.89	1.18	69.67
0.76	3.37	1.02	69.73
0.81	2.97	0.93	68.69
0.86	2.63	0.83	68.44
0.91	2.36	0.74	68.64
0.96	2.10	0.68	67.62
1.01	1.89	0.62	67.20

From table III it is deduced that high reductions of the magnetic field can be obtained in the vicinity of the single-phase line by using a pure-iron shield with a thickness of just 0,5 mm.

Figure 6 displays the magnetic field intensities shown in table III.

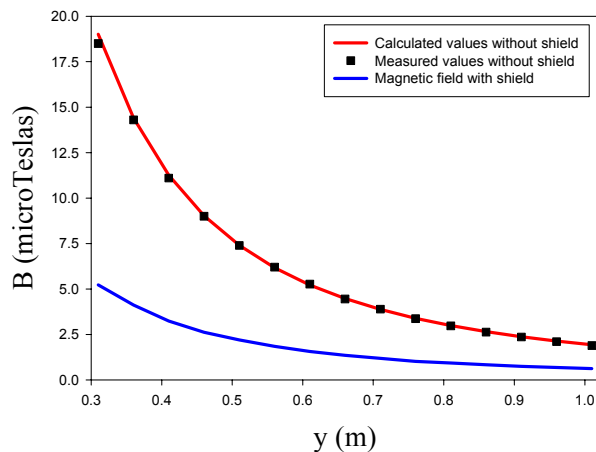


Figure 6. Values of the magnetic field in the (0,y) points, with shield and without shield.

8. Conclusions

Once the study has been realized, the following conclusions can be deduced:

- It has been shown that not expensive shielding materials as pure-iron are able to be used for shielding the B fields generated by a single-phase power line.
- The theoretical values generated by the single-phase line are very close to the measures made in this work.
- The measurements realized in this work show that when dealing with a pure-iron cylindrical shield with a thickness of 0,5 mm, the magnetic fields values near the single-phase power line are reduced approximately in a factor of 70 %.
- In future works we will research other not expensive soft ferromagnetic materials that can be used to build very effective magnetic shields.

References

- [1] IARC. IARC finds limited evidence that residential magnetic fields increase risk of childhood leukaemia. www.iarc.fr, cie@iarc.fr, june 2001.
- [2] Handbook of Chemistry and Physics, 70th. Edition. CRC Press, pp. E-128, 1989-90.
- [3] Fahy S., Kittel C. y Louie S. "Electromagnetic screening by metals". Am. J. Phys. Vol 11, pp. 989 (1988).
- [4] P. Rochon and N. Gauthier "Strong shielding due to an electromagnetically thin metal sheet". Am. J. Phys. Vol. 58, pp. 276 (1990).
- [5] J.R. Riba, X. Alabern. "Reducción del campo magnético creado por líneas enterradas de alta tensión utilizando materiales no ferromagnéticos" in Proc. 8CLEE 2003, Vol. 1, pp. 1.149-1.154.
- [6] Jordi-Roger Riba, Xavier Alabern. "Estudio de los campos magnéticos y eléctricos generados por una línea aérea de 220 kV". 7as. Jornadas "La Ingeniería Eléctrica y Ambiental en el siglo XXI", INGENA 2001. Proceedings, P071, pg. 219-223. Universidad de Cantabria, Santander, 2001.
- [7] Jordi-Roger Riba, Xavier Alabern. "Campo magnético generado por las líneas de alta tensión. Efecto del grado de desequilibrio del sistema de corrientes trifásicas". 7as. Jornadas Hispano-Lusas de Ingeniería Eléctrica. Proceedings, Vol. II, pg. 43-48. Universidad Carlos III, Leganés (Madrid), 2001.
- [8] Gao Yougang, Yu Lifang. Determination of Dangerous Region of the Electromagnetic Pollution Caused by the Electric Fields around Power Lines. International Conference on Communication Technology (ICCT 98), pgs. S26-01-1 a S26-01-4, 22-24, October 1998, Beijing (China).
- [9] P.S. Wong, M.A. Janoska, C. Light, R.W. McCourt. "Long Term Magnetic Field Monitoring Near Power Lines". IEEE Transactions on Power Delivery, 12 (2), 922-927, 1997.
- [10] W.T. Kaune, L.E. Zafanella. "Analysis of Magnetic Fields Produced Far From Electric Power Lines". IEEE Transactions on Power Delivery, 7 (4), 2082-2091, 1992.